Seismic Design of Friction-Damped Braced Frames Based on Historical Records

Robert Levy,[a] Oren Lavan,[b] and Avigdor Rutenberg,[c] M.EERI

This paper is concerned with the design of friction dampers designed to slip at a predetermined level and dissipate a substantial portion of the seismic energy, leaving the structure practically intact without its members having to yield or buckle. They are appropriate for use in seismic design of new buildings and in retrofitting existing structures. By choosing a practical design requirement rather than minimizing some energy criterion, a novel design procedure attains the stiffness of the individual braces and their displacements at the threshold of activation. The procedure is a two-phase process that uses in Phase 1 an equivalent single-degree-of-freedom (SDOF) system to obtain an optimal natural period of the structure by performing a full nonlinear dynamic analysis for a set of earthquake records. Phase 2 then enforces the same first mode on both the braced and unbraced frames, with the aim of ensuring simultaneous slippage. The procedure was applied to a 10-story steel frame. It yielded a rather technically attractive design of the braces since for close to mean plus standard deviation of the records, the resulting maximum roof displacements fell within the allowable design, as initially constrained to, and simultaneous slip of all braces occurred for most records. This procedure is rather simple in that the main computational effort, i.e., nonlinear analysis needed for Phase 1, is performed on an equivalent SDOF system only, whereas analysis of the multi-degree-of-freedom (MDOF) system is a linear eigenvalue analysis. [DOI: 10.1193/1.1950674]

INTRODUCTION

The heavy damage caused by the 1994 Northridge and the 1995 Kobe earthquakes has accelerated the re-examination of the time-honored philosophy that life safety should be the only criterion for the design of structures under strong earthquakes. Damage limitation is now becoming a design objective. The need to contain damage also leads to a re-examination of the traditional design approach in which dissipation of seismic energy is achieved through limited damage in the post-elastic range of selected structural elements. Hence the increasing interest in mechanical energy dissipating devices. The need for such devices is more acute in concentrically braced frames, since the ability of the diagonal braces to dissipate energy in severe earthquakes is limited mainly

[a] Associate Professor, Faculty of Civil Engineering, Technion–Israel Institute of Technology, Technion City, Haifa 32000, Israel; e-mail: cvrlevy@tx.technion.ac.il; fax: 972 4 8295697
[b] Ph.D. Candidate, Faculty of Civil Engineering, Technion–Israel Institute of Technology, Technion City, Haifa 32000, Israel; e-mail: lavan@tx.technion.ac.il
[c] Professor Emeritus, Faculty of Civil Engineering, Technion–Israel Institute of Technology, Technion City, Haifa 32000, Israel; e-mail: avrut@tx.technion.ac.il

by their tensile yielding and by the buckling capacity. The fundamental underlying principles for the design of energy dissipating devices of various kinds and their actual implementation can be found in the comprehensive book by Constantinou, Soong, and Dargush (1998).

Friction dampers, which are designed to slip at a predetermined force level, were studied by Filiatrault and Cherry (1987, 1990). Friction devices that utilize slotted bolted connections (SBCs) where, basically, high-strength bolts connect two parts of a brace, were proposed by Fitzgerald (1989). Popov et al. (1993) also applied SBCs to a flexible experimental model that they tested on a shaking table, and found them quite effective in dissipating most of the input energy. Constantinou et al. (1991) developed and tested a displacement controlled device that consisted of a spring and frictional assemblies. The frictional assembly used graphite-impregnated bronze plates with stable hysteresis loops and, under earthquake motions, was found to perform as designed. Devices with cobalt surfaces were successfully tested by Tremblay and Stiemer (1993). Friction dampers that slide against walls of steel cylinders were described by Aiken and Kelly (1993) and Nims et al. (1993). Kitajima et al. (1997) tested a RC frame retrofitted with friction dampers that showed a stable hysteresis. Ohnishi et al. (1999) tested a damper consisting of a copper alloy rod and an alloy tool steel die and found the hysteresis loops to be stable under nonstationary excitations. Friction dampers were implemented, mostly in Canada, as braces in retrofitted and new steel structures by Pall (e.g., Pall and Pall 1996, and references therein). The Sumitomo devices (Aiken and Kelly 1990) were installed in two buildings in Japan, and SBCs were used to retrofit two buildings in Stanford. Hanson and Soong (2001) described the 13-story TransWorld Bank concrete-frame–structure upgrade using friction dampers, designed by Way and Taylor (1996).

Design methodologies for optimal frame retrofitting using friction dampers were proposed by several researchers (Pall and Marsh 1982, Filiatrault and Cherry 1989, Vulcano 1995, Gluck et al. 1996, Singh and Moreschi 2001). These methodologies minimized different performance indices rather than aiming at a specified target performance index. Also proposed in the literature are design methodologies that are based on the condensation of the multi-degree-of-freedom (MDOF) structure to a single-degree-of-freedom (SDOF) system (Vulcano 1995, Rao et al. 1996, Fu and Cherry 2000, Levy et al. 2001). The condensation techniques presented in these papers do not require the same first modes for the braced and bare frames, and hence are not likely to lead to simultaneous slippage of the dampers, which is essential for the condensation to be accurate. A methodology for the design of frame retrofitting using friction dampers for a target performance index ensuring simultaneous slippage of the dampers is not yet available.

The present paper proposes a design procedure for friction dampers, i.e., the evaluation of the stiffness of the individual braces and their elongation at slip threshold, for a wide range of earthquake records, while constraining the drifts to result in the first-mode displacement shape of the frame. The procedure is applicable to the seismic design of new frames and for retrofitting existing ones, particularly those with limited available ductility.

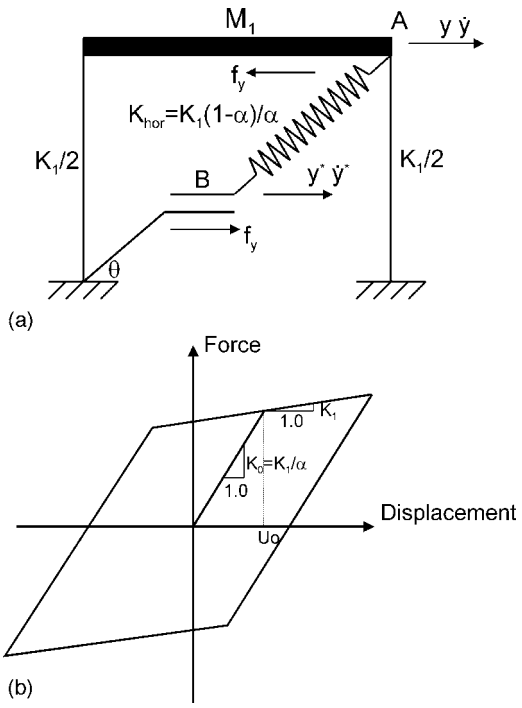

Figure 1. (a) Analytical model of one-story friction-braced frames, and (b) bilinear hysteresis diagram.

As for the actual earthquake motions, a mixed set of 35 earthquake records representing a wide range of possible excitations grouped according to their ratio of peak ground acceleration (PGA) to peak ground velocity (PGV) was used for design (Naumoski et al. 1993). However, the actual choice of earthquakes is up to the designer.

THEORETICAL BACKGROUND

This section presents a two-phase design methodology that, basically, ensures that the first modes of both the braced and unbraced frames are the same and constraints the drifts. The dynamic model, which is given in some detail in Levy et al. (2001), is summarized below.

DYNAMIC BEHAVIOR

The one-story SDOF equivalent model of the multistory frame (Figure 1a) consists of a linear flexural frame having stiffness K_1 and mass M_1; a linear spring having horizontal stiffness $K_{\text{br,hor}}=K_1(1-\alpha)/\alpha$ (α=secondary slope ratio, Figure 1b); and a Coulomb slip element modeling the diagonal brace and its slipping device. A stick stage and a sliding stage describe the motion of the brace. The stick stage has the velocity of the friction damper $\dot{y}^*$ equal to zero, the stiffness of the frame equals the initial stiffness of

the braced frame, and the friction force is equal to the instantaneous horizontal component of the force in the brace. Linear behavior is assumed at this stage. In the sliding stage the velocity of the friction damper $\dot{y}^*$ equals that of the frame $\dot{y}$. The stiffness of the braced frame is now that of the frame without the brace, and the friction force equals the slip force in the brace. Here, too, linear behavior of the unbraced frame is assumed. When the direction of the horizontal movement of the frame is reversed, the system returns to the first stage. Note that linear behavior is a somewhat restrictive assumption, the validity of which should be assessed at the end of the analysis, and remedial steps, such as decreasing the nominal displacement, should be taken if the assumption is not met.

The equation of motion of the SDOF bilinear hysteretic system describing a MDOF system is

$$\ddot{y}(t) + 2\xi\omega\dot{y}(t) + \alpha\omega^2 y(t) + (1-\alpha)\omega^2(y(t) - y^*(t)) = -\Gamma a(t) \tag{1}$$

in which $y(t), \dot{y}(t), \ddot{y}(t)$=displacement, velocity, and acceleration of the frame, respectively; $y^*(t)$=slip displacement of friction damper; $a(t)$=earthquake acceleration at the base; α=secondary slope ratio in the hysteretic model (Figure 1b), i.e., the stiffness of the unbraced frame divided by the stiffness of the braced frame; ξ=viscous damping ratio; ω=natural frequency of the SDOF structure, and Γ=modal participation factor.

The generalized differential equation of motion for the MDOF braced frame can be expressed as follows:

$$\mathbf{M}\ddot{\mathbf{y}}(t) + \mathbf{C}\dot{\mathbf{y}}(t) + \mathbf{K}(\mathbf{y}, \dot{\mathbf{y}})\mathbf{y}(t) + \mathbf{f}_\mathbf{y} = -a(t)\mathbf{M}\mathbf{i} \tag{2}$$

where $\mathbf{y}(t), \dot{\mathbf{y}}(t), \ddot{\mathbf{y}}(t)$=displacement, velocity, and acceleration vectors for the story levels, respectively; **M**, **C**, and **K** are, respectively, the mass, damping, and stiffness matrices of the unbraced structure; $\mathbf{f}_\mathbf{y}$=vector of horizontal components of friction forces that can take values of − slip force to + slip force; and **i**=vector whose entries are unity. The solution of the set of Equations 2 is performed using RUAUMOKO (Carr 2000).

DESIGN PROCEDURE

The design of friction dampers consists of evaluating the stiffness of the braces and their slip elongations for a given set of constraints, as shown subsequently. The design procedure has two main phases.

In Phase 1 the MDOF frame is condensed into an equivalent SDOF model and a brace is designed, i.e., the secondary slope ratio α is determined. Thus an equivalent natural period of the SDOF braced model, T_{br}, is obtained. This is the period for which the MDOF frame is designed in Phase 2. Brace stiffnesses and slip elongations of the MDOF frame are produced in Phase 2 such that the natural period of the braced frame equals the period, T_{br}, of Phase 1. Basic to the procedure is one main assumption, which is usually valid for low-rise frames, that the response of the bare frame exhibits first-mode behavior. A detailed description of the two-phase procedure follows.

Phase 1

Condensation of the MDOF frame to an equivalent SDOF model for which the mass, secondary stiffness, slip elongation, and nominal displacement are computed necessitates, in addition to first-mode behavior, that the bare and braced frames possess identical first mode. Having identical first-mode shapes enables simultaneous slippage to be enforced under single mode (first-mode) behavior. This requirement is achieved in Phase 2. The primary stiffness of the SDOF braced model, and hence its period, T_{full}, is determined such that the desired constraints on the displacements of the SDOF model, representing the actual constraints on the roof displacements of the MDOF frame, are satisfied.

In this work, two roof displacements are of interest. They are referred to as the nominal and the allowable roof displacements. The nominal displacement is determined from a pushover analysis on the bare frame for the first-mode load pattern. It is defined as the maximum roof displacement for which the load displacement behavior remains linear. Associated with the nominal displacement is a design requirement that the sum of the squares of the deviations from the permissible nominal displacement of the maximum displacements for all the records be minimized. Such a design requirement does not necessarily prevent a large scatter around the nominal displacement, and thus may lead to many earthquakes causing roof displacements larger than a reasonable allowable displacement. The allowable displacement is tied to the nominal displacement by a desired factor greater than 1.0. In this work the factor was chosen as 1.2 so that $\Delta^{\text{allowable}} = 1.2\Delta^{\text{nominal}}$. Associated with the allowable displacement is a requirement that the mean (M)+standard deviation (SD) of the maximum roof displacement should not exceed the allowable displacement for all the records. Note that requiring a much stricter constraint, say M+2SD, for the same allowable displacement will lead to much stiffer braces, which in turn might strongly affect column and foundation response. Only one of the two design requirements will be active. When the nominal displacement criterion is active (as is the case of the numerical example) it is to be expected that the mean displacement shape from a nonlinear analysis on the MDOF system will closely match the first-mode shape of the bare frame scaled to the nominal roof displacement. When the allowable roof displacement criterion is active it is expected that the mean displacement shape will have values smaller than that. The analysis in Phase 1 is actually a full SDOF nonlinear analysis using the dynamic model of Equation 1.

Assuming that all the friction dampers are activated simultaneously, and the first-mode shape of the braced frame is that of the bare frame, the mass, secondary stiffness, slip elongation, and nominal displacement of the equivalent SDOF model can be computed as follows (e.g., *FEMA-365* [ASCE 2000], Krawinkler and Seneviratna 1998):

$$M_1 = \boldsymbol{\phi}_1^{\mathrm{T}} \cdot \mathbf{M} \cdot \mathbf{1} \tag{3}$$

$$K_1 = \boldsymbol{\phi}_1^{\mathrm{T}} \cdot \mathbf{K}_{\text{frame}} \cdot \boldsymbol{\phi}_1 \cdot \frac{\boldsymbol{\phi}_1^{\mathrm{T}} \cdot \mathbf{M} \cdot \mathbf{1}}{\boldsymbol{\phi}_1^{\mathrm{T}} \cdot \mathbf{M} \cdot \boldsymbol{\phi}_1} \tag{4}$$

$$U_o = u_{o,roof} \cdot \frac{\phi_1^T \cdot \mathbf{M} \cdot \phi_1}{\phi_1^T \cdot \mathbf{M} \cdot \mathbf{1}} \tag{5}$$

$$\Delta_1^{nominal} = \Delta^{nominal} \cdot \frac{\phi_1^T \cdot \mathbf{M} \cdot \phi_1}{\phi_1^T \cdot \mathbf{M} \cdot \mathbf{1}} \tag{6}$$

where ϕ_1 is the first-mode shape of the frame normalized with respect to roof displacement; $u_{o,roof}$=roof displacement of the MDOF frame at slip; U_o=slip elongation of the SDOF model; $\Delta^{nominal}$=nominal roof displacement in the MDOF frame; and $\Delta_1^{nominal}$ =SDOF nominal displacement. Although the condensation made here also leads to a reasonable prediction of the MDOF response when the first-mode shape does not remain constant throughout the analysis (*FEMA-365*), it is emphasized here that the mode shape of the frame, before and after slippage, will be enforced in Phase 2 to be exactly the same.

The maximum slip elongation of the braces in the MDOF frame should not exceed their yield elongation, u_y, assuming buckling is restrained. Hence the maximum allowed horizontal component of the slip elongation of a single brace, $u_{0,max}$, is taken as $u_{0,max} = u_y = (f_s l \cos\theta)/EA$. Here $f_s = \sigma_y A$=maximal slip force (σ_y=yield stress); l=length of the brace; E=Young's modulus; A=cross sectional area of brace; and θ=angle of brace inclination (see Figure 1a). Assuming first-mode shape response the roof displacement at slip, $u_{o,roof}$, becomes $u_{0,max}$ multiplied by the first-mode roof displacement ordinate (1.0) divided by the first-mode maximum drift, δ_{max1}, (see Figure 2), and is given by

$$u_{o,roof} = u_{o,max} \frac{1.0}{\delta_{max\,1}} \tag{7}$$

where $\delta_{max1} = (\phi_{i1} - \phi_{(i-1)1})_{max}$ and ϕ_{i1} is the ith element of ϕ_1.

The period, T_{full}, of the equivalent **braced** SDOF structure is obtained as follows:

- *Step 1:* Perform a nonlinear SDOF analysis (Equation 1 with $\Gamma = 1$) to evaluate the maximum response for a given set of time histories, with mass M_1 (Equation 3), secondary stiffness K_1 (Equation 4), and slip elongation U_0 (Equation 5) for α values ranging from 0.0^+ to 1.0.
- *Step 2:* Calculate α^*, the optimum value of α in the range of 0.0^+ to 1.0 for which the objective function $\Sigma_{i=\text{all records}}(\Delta_1^i - \Delta_1^{nominal})^2$ is minimized while satisfying the constraint of $(M(\Delta_1^i) + SD(\Delta_1^i)) \leq \Delta_1^{allowable}$. Here Δ_1^i is the maximum displacement of the SDOF model excited by record i, and $\Delta_1^{nominal}$ is the nominal displacement stipulated for the SDOF model.
- *Step 3:* Calculate the period of the MDOF braced frame for design in Phase 2 as (Figure 1b)

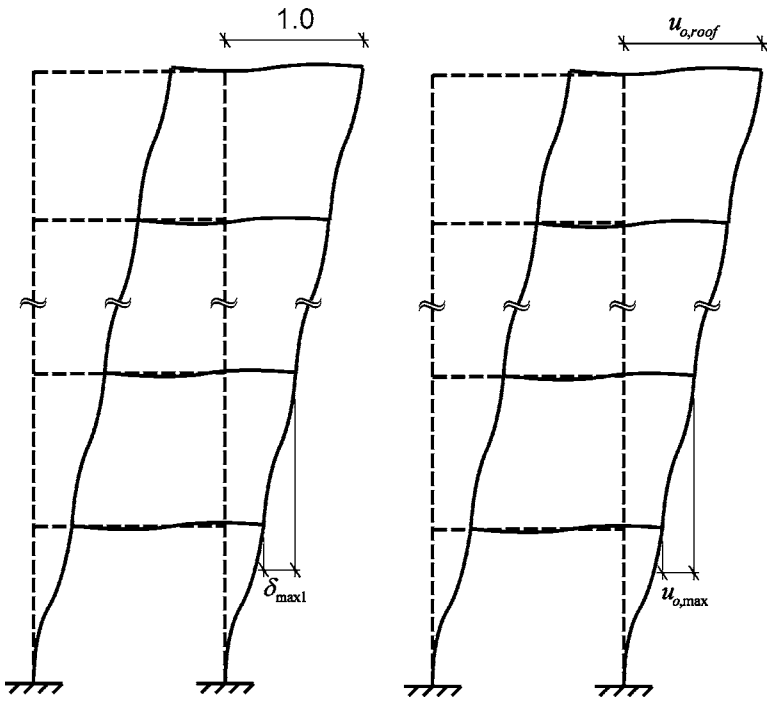

Figure 2. $u_{o,roof}$ determination.

$$T_{full} = 2\pi\sqrt{\frac{M_1\alpha^*}{K_1}} \tag{8}$$

This is the period for which the braced frame is designed.

Phase 2

The design procedure of Phase 2 should produce the brace stiffnesses and the slip elongations while satisfying two demands. The first is that the period of the braced frame should equal the period, T_{full}, of Phase 1. The second is that the first-mode shape of the braced frame should be that of the bare frame to result in simultaneous slippage in all the friction dampers.

Under the conditions that the first-mode shape of the braced frame is the same as that of the bare frame, and that the response is controlled by the first mode, simultaneous slip will occur if the slip elongation of the braces is proportional to the first-mode interstory drifts. This is enforced by computing the slip elongations of the braces from

$$u_{0_i} = \frac{\delta_{i1}}{\delta_{\max 1}} u_{0,\max} \tag{9}$$

where $\delta_{i1} = \phi_{i1} - \phi_{(i-1)1}$ and $u_{0,\max}$ is the maximum slip elongation of a single brace.

The other two demands of Phase 2, i.e., the design should yield the period, T_{full}, of Phase 1, and the first-mode shape of the braced frame should be the same as that of the bare frame, are enforced from

$$[\mathbf{K}_{\text{frame}} + \mathbf{K}_{\text{br}}]\boldsymbol{\phi}_{\mathbf{1}} = \omega_{\text{full}}^2 \mathbf{M}\boldsymbol{\phi}_{\mathbf{1}} \tag{10}$$

or

$$\mathbf{K}_{\text{br}}\boldsymbol{\phi}_{\mathbf{1}} = \lfloor \omega_{\text{full}}^2 \mathbf{M} - \mathbf{K}_{\text{frame}} \rfloor \boldsymbol{\phi}_{\mathbf{1}} \tag{11}$$

where $\omega_{\text{full}} = 2\pi / T_{\text{full}}$ and $\mathbf{K}_{\text{br}}$ is the stiffness matrix of the braces (assuming that the additional axial deformations due to the change in the manner of shear transfer from shear forces in the columns to axial forces in the bracings can be neglected). Using the following transformation from displacements DOFs to drifts DOFs:

$$\boldsymbol{\phi}_1 = \mathbf{T}\boldsymbol{\delta}_1; \quad \mathbf{T} = \begin{bmatrix} 1 & 0 & 0 & 0 \\ 1 & 1 & 0 & 0 \\ \vdots & \vdots & \ddots & 0 \\ 1 & 1 & 1 & 1 \end{bmatrix} \tag{12}$$

The mass and stiffness matrices take the form

$$\bar{\mathbf{M}} = \mathbf{T}^{\text{T}}\mathbf{M}\mathbf{T}; \bar{\mathbf{K}}_{\text{frame}} = \mathbf{T}^{\text{T}}\mathbf{K}_{\text{frame}}\mathbf{T}; \quad \bar{\mathbf{K}}_{\text{br}} = \mathbf{T}^{\text{T}}\mathbf{K}_{\text{br}}\mathbf{T} \tag{13}$$

Thus the stiffness matrix of Equation 11 transforms from a tri-diagonal to a diagonal matrix as

$$\begin{bmatrix} k_{\text{br},1} & 0 & 0 & 0 \\ 0 & k_{\text{br},2} & 0 & 0 \\ 0 & 0 & \ddots & 0 \\ 0 & 0 & 0 & k_{\text{br},N} \end{bmatrix} \begin{Bmatrix} \delta_{1,1} \\ \delta_{2,1} \\ \vdots \\ \delta_{N,1} \end{Bmatrix} = [\omega_{\text{full}}^2 \bar{\mathbf{M}} - \bar{\mathbf{K}}_{\text{frame}}]\boldsymbol{\delta}_1 \tag{14}$$

or

$$\begin{bmatrix} \delta_{1,1} & 0 & 0 & 0 \\ 0 & \delta_{2,1} & 0 & 0 \\ 0 & 0 & \ddots & 0 \\ 0 & 0 & 0 & \delta_{N,1} \end{bmatrix} \begin{Bmatrix} k_{\text{br},1} \\ k_{\text{br},2} \\ \vdots \\ k_{\text{br},N} \end{Bmatrix} = [\omega_{\text{full}}^2 \bar{\mathbf{M}} - \bar{\mathbf{K}}_{\text{frame}}]\boldsymbol{\delta}_1 \tag{15}$$

Since for framed structures it is not reasonable to assume that the drift ordinates of the first mode are not positive, the coefficient matrix is not singular, thus Equation 15

has a unique solution for the vector of brace stiffnesses $\mathbf{k}_{br}$. Substituting the eigenvalue equation of the bare frame, $\bar{\mathbf{K}}_{frame}\boldsymbol{\delta}_1 = \omega_1^2\bar{\mathbf{M}}\boldsymbol{\delta}_1$, in Equation 15, where ω_1 is the first-mode natural frequency of the bare frame, leads to

$$\begin{bmatrix} \delta_{1,1} & 0 & 0 & 0 \\ 0 & \delta_{2,1} & 0 & 0 \\ 0 & 0 & \ddots & 0 \\ 0 & 0 & 0 & \delta_{N,1} \end{bmatrix} \begin{Bmatrix} k_{br,1} \\ k_{br,2} \\ \vdots \\ k_{br,N} \end{Bmatrix} = [\omega_{full}^2 - \omega_1^2]\bar{\mathbf{M}}\boldsymbol{\delta}_1 \tag{16}$$

Since all the components of $\bar{\mathbf{M}}$ and $\boldsymbol{\delta}_1$ are positive, the components of the vector $\bar{\mathbf{M}}\boldsymbol{\delta}_1$ are positive as well, hence (for $\omega_{full}^2 > \omega_1^2$) the components of the vector on the LHS of Equation 16 are positive. Recalling that the elements of the diagonal coefficient matrix on the LHS of Equation 16 are positive leads to the conclusion that the components of $\mathbf{k}_{br}$ are also positive. Thus computing the brace stiffnesses from Equation 15 leads to positive and unique stiffnesses for the braces and to the desired first-mode shape of the braced frame, while its period equals T_{full}.

As is evident from the preceding formulation, the procedure assumes that the bare frame, and hence its SDOF proxy, behave during the earthquake practically elastically up to the nominal diplacement. This, of course, has to be verified prior to the analysis, say, by means of pushover analysis having the first-mode shape as the load pattern.

SELECTION OF EARTHQUAKE RECORDS

Strong motion earthquake records are basic data for the engineer. A study of such records can give insight into the nature of earthquake ground shaking. When used as input for experiments or analyses, they present realistic simulation for studying the nature of the structural response to seismic excitation. Earthquake ground motion records can be used to evaluate the performance of a particular structure, or assess the adequacy of building code requirements. One major parameter that has significant effect on the structural response is the frequency content of the record. For estimation of the frequency content, a simple approach based on the peak ground acceleration to peak ground velocity ratio (A/V ratio) is used (Heidebrecht and Lu 1988, Naumoski et al. 1993). Motions with high A/V ratios usually represent near earthquakes, whereas those with low A/V are usually due to distant strong events.

The Naumoski et al. (1993) report describes five ensembles of 15 earthquake records, each having been assembled to defined ranges of A/V ratios. The ensembles are categorized herein as High (VH: A/V = 2.63–3.52), New High (NH: A/V = 1.60–2.43), New Intermediate (NI: A/V = 0.82–1.21), New Low (NL: A/V = 0.62–0.79), and New Very Low (NVL: A/V = 0.36–0.59). Note that A is in units of *g* and V is in m/sec.

This work uses 35 (12 from the NVL, 12 from NI, and 12 from NH categories) out of the 75 records. These are identified according to the record numbers given in the Naumoski et al. (1993) report, and presented in Table A1 of the Appendix. The normaliza-

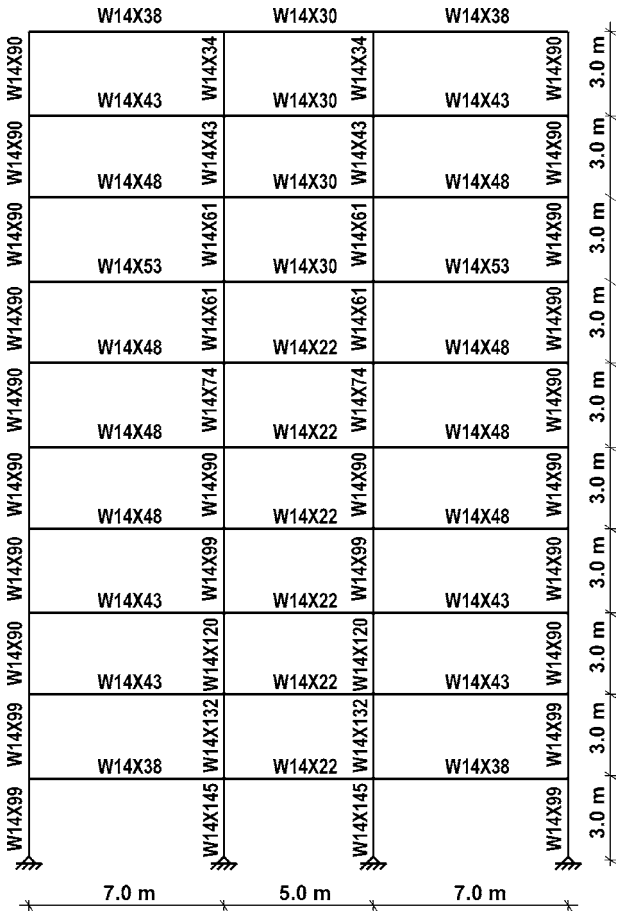

Figure 3. A 10-story, 3-bay steel frame for the example.

tion rule used in this work scales *all* the records to PGV=0.4 msec (seismic risk Zone 4), a scaling procedure used in the Canadian seismic code (Associate Committee 1995).

DESIGN OF FRICTION DAMPERS FOR A 10-STORY STEEL FRAME

RESULTS

An existing industrial building consisting of a symmetric 10-story, 3-bay steel frame (Figure 3) is used as an example for which the braces (stiffnesses and slip elongations) are to be designed. The central bay, on which the braces are to be implemented, is 5.0 m wide and 3.0 m high, hence the braces' length is $L=5.83$ m and the angle between the braces and story levels $\theta=30.96°$. Each story has a mass of 54.0 tons, and the unbraced stiffness matrix K_{frame} (ton/cm) of the structure is given below for the condensed ten horizontal degrees of freedom (numbered upwards from the first floor to the roof).

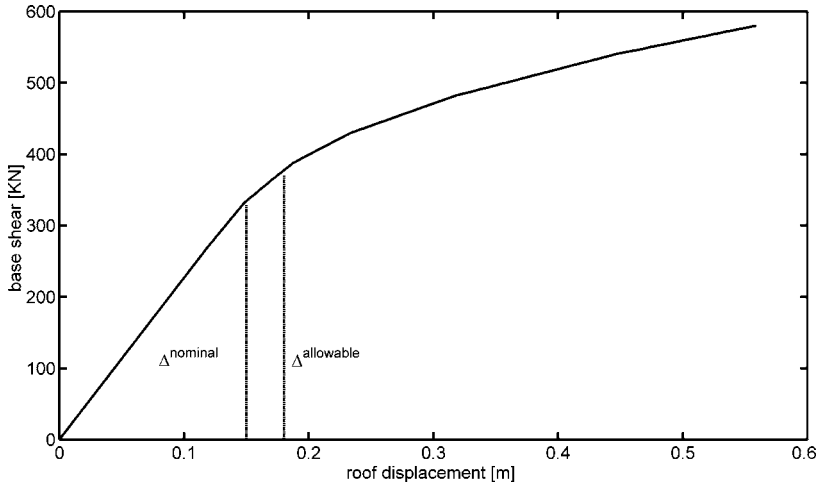

Figure 4. Force displacement curve for first-mode load pattern (pushover analysis).

$$\mathbf{K}_{frame} = \begin{bmatrix} 146.16 & -124.89 & 36.66 & -5.53 & 1.14 & -0.29 & 0.08 & -0.02 & 0.00 & -0.00 \\ -124.89 & 191.20 & -126.18 & 36.62 & -6.09 & 1.27 & -0.29 & 0.09 & -0.02 & 0.00 \\ 36.66 & -126.18 & 183.86 & -120.84 & 35.28 & -6.13 & 1.30 & -0.28 & 0.08 & -0.01 \\ -5.53 & 36.62 & -120.84 & 176.52 & -116.51 & 34.22 & -6.19 & 1.33 & -0.28 & 0.06 \\ 1.14 & -6.09 & 35.28 & -116.51 & 169.43 & -110.97 & 32.90 & -6.14 & 1.24 & -0.19 \\ -0.29 & 1.27 & -6.13 & 34.22 & -110.97 & 161.92 & -106.31 & 31.09 & -5.77 & 0.88 \\ 0.08 & -0.29 & 1.30 & -6.19 & 32.90 & -106.31 & 156.37 & -102.79 & 29.00 & -4.04 \\ -0.02 & 0.09 & -0.28 & 1.33 & -6.14 & 31.09 & -102.79 & 147.34 & -90.53 & 19.94 \\ 0.00 & -0.02 & 0.08 & -0.28 & 1.24 & -5.77 & 29.00 & -90.53 & 115.35 & -49.09 \\ -0.00 & 0.00 & -0.01 & 0.06 & -0.19 & 0.88 & -4.04 & 19.94 & -49.09 & 32.41 \end{bmatrix}$$

Phase 1 uses the fundamental period (T=2.61 sec) of the bare frame for the equivalent SDOF frame. The nominal displacement is 15.0 cm. Pushover analysis for the first-mode load pattern indicated no plastic behavior for lower values of roof displacement (see Figure 4). The horizontal component of the maximum allowable slip elongation of each brace, $u_{0,\max}=f_y L \cos 30.96^0/E=2375\times 583\times 0.8575/2.05\times 10^6=0.58$ cm. The slip elongation for the "equivalent" SDOF is taken as $u_{o,roof}=u_{o,max}/\delta_{max1}=0.58/0.207=2.8$ cm. The participation factor $\Gamma=1.0$ was used for the first mode of the unbraced frame. The 9 records for which the maximum displacement of the bare frame, i.e., $\alpha=1.0$ was less than $\Delta^{nominal}$, were omitted from the analysis. These records are marked with an asterisk in Table A1. The optimal α is 0.16, calculated according to **Phase 1** (in the $\Delta^{nominal}$ coordinate system). Figure 5 displays four curves of interest for the choice of α^*. Curves 1, 2, 3, and 4 show, respectively, the change with α of the objective function

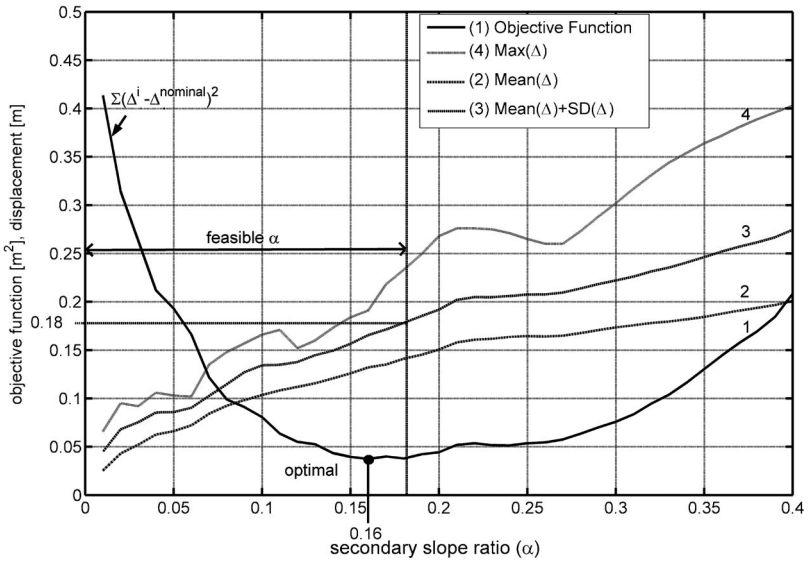

Figure 5. Graphical determination of secondary slope ratio.

$\Sigma_{i=\text{all records}}(\Delta^i - \Delta^{\text{nominal}})^2$, the mean roof displacement, the mean roof displacement plus one standard deviation, (M+SD), and the maximum roof displacement. The value of $\alpha^* = 0.16$ was the lowest point of Curve 1 satisfying the constraint that the M+SD displacement (Curve 3) for that value of α is less than $\Delta^{\text{allowable}} = 18.0$ cm.

In Phase 2 the design process is continued according to Equation 15 and Equation 9 to yield results summarized in Table 1. A full nonlinear analysis of the MDOF system with friction dampers is now performed using RUAUMOKO (Carr, 2000) and the M and

Table 1. Brace stiffnesses and slip elongations of the friction dampers

story #	u_0 horizontal slippage (cm)	brace stiffness (ton/cm)	slip forces (ton)
1	0.58	64.83	43.77
2	0.45	81.61	42.47
3	0.38	91.79	40.17
4	0.33	97.28	37.04
5	0.28	100.22	33.18
6	0.24	100.75	28.68
7	0.20	103.26	23.63
8	0.15	104.40	18.14
9	0.11	92.27	12.33
10	0.08	68.89	6.25

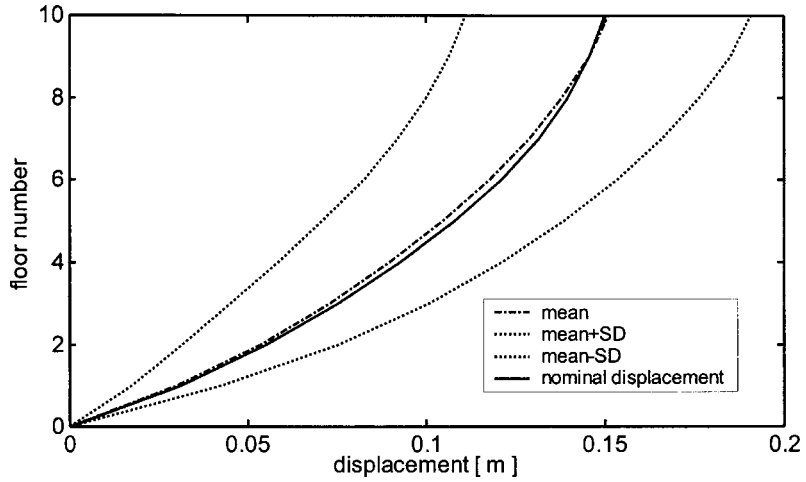

Figure 6. Deformed shape at top-story displacement: full nonlinear analysis with friction dampers.

M±SD story displacements are displayed in Figure 6 in three curves. A fourth curve in Figure 6 shows the nominal displacement, which actually is the first-mode shape of the bare frame scaled to the nominal roof displacement. It can be seen from Figure 6 that, as expected, the mean deformed shape of the friction-damped braced frame practically matches the targeted first-mode shape of the bare frame, and thus the assumption of first-mode behavior is verified. Figure 7 shows the nominal and the M and M±SD drifts, and Figure 8 shows the deformed shapes at maximum roof displacements. The nominal

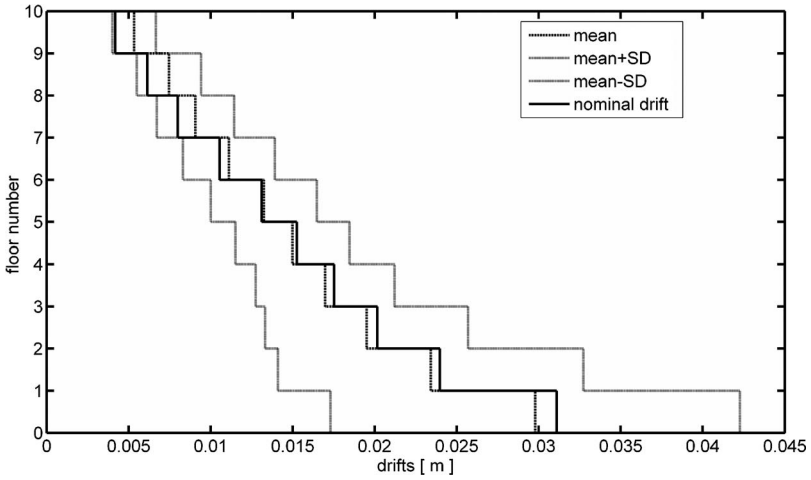

Figure 7. Drifts at maximum roof displacement: full nonlinear analysis with friction dampers.

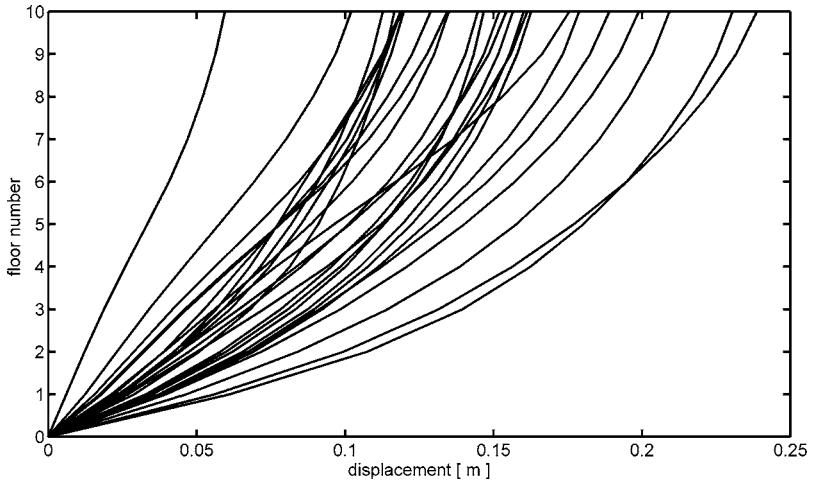

Figure 8. Deformed shapes for all 26 records at maximum roof displacement: full nonlinear analysis with friction dampers.

drift is obtained from the first-mode shape drifts scaled to the nominal roof displacements. The results of Figure 8 show that 5 out of the 26 records (19.2%) caused a maximum displacement greater than $\Delta^{\text{allowable}}$. These records are from Friuli 1976, Mexico City 1985 (2 components), Loma Prieta 1989, and Kern County 1940.

As can be seen, the nominal displacement criterion was the one active in this example, yet the second criterion was not satisfied because the M+SD roof displacement of the braced frame (19 cm from Figure 6) was slightly greater than $\Delta^{\text{allowable}}$. This result may be justified considering that higher mode effects have not been included, and that the MDOF scatter of roof displacements is likely to be larger than that of their SDOF counterparts.

Figure 9 shows the deformed shapes of the bare frame under the same excitations. It is evident that the bracings lowered the displacements appreciably. Note, however, that limited yielding of several beams in the braced frame was observed for some records.

CONCLUSIONS

An efficient methodology was presented for the design of friction dampers as supplemental braces to a given MDOF bare frame for a given nominal roof displacement. Nonlinear time-history analysis of the damped frame shows a mean deformed shape that practically matches the targeted first-mode shape of the bare frame (Figures 6 and 7). Moreover, it can be observed from Figures 8 and 9 that the deformed shapes of the braced frame have a closer resemblance to the first mode than those of the bare frame. This may be due to the dampers acting as filters to higher modes.

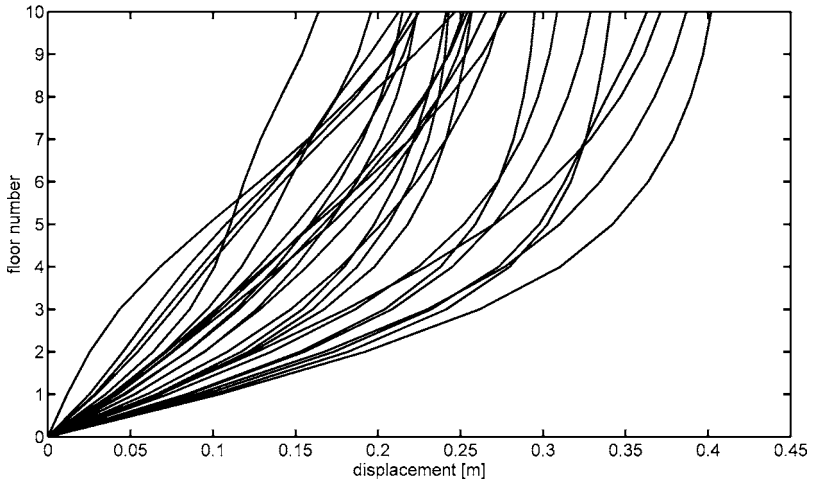

Figure 9. Deformed shapes for all 26 records at maximum roof displacement: full nonlinear analysis without friction dampers.

Phase 1 of the two-phase methodology performs nonlinear calculations on an equivalent condensed SDOF frame, the legitimacy of which was based on first-mode behavior. The analytical approach of Phase 2 for the distribution of brace stiffnesses and slip elongations is novel and unique and easily implemented through eigenvalue considerations.

The braced frame exhibited linear elastic behavior for most records. This was targeted and practically achieved by the choice of allowable drifts and roof displacements using pushover analysis for a first-mode load pattern.

The use of a realistic ensemble of time histories with different frequency characteristics and scaled to match the expected peak ground velocity at the site yields a reasonable practical design since, as Figure 8 indicates, 100% of the records are within 133% of the allowable design, 90% within 117% and 80.7% within 100%.

Predicting the deviations of the MDOF displacements from first-mode results is not easy, and depends on many factors (Chopra et al. 2001). Hence, a strategy that lowers the nominal displacement by a judiciously chosen factor that takes into account the possibility that the expected multi-to-single degree displacement ratio is larger than 1.0, as is the case in the numerical example, could lead to even better results.

Regarding simultaneous slippage, the mean displacement curve and the first-mode curve are practically identical (Figure 6), hence simultaneous slippage has occurred in the mean. Moreover, as has been observed, for most of the individual runs this was in fact the case.

APPENDIX

This appendix lists in table form (Table A1) the earthquake records used in this paper. More details on the records are found in Naumoski et al. (1993). Records marked with an asterisk were discarded because they produced a maximum roof displacement of the bare frame that was less than the target roof displacement for the braced frame.

Table A1. Description of earthquake records

Earthquake	Record number	Mean A/V ratio	Epicentral Distance (km)
Long Beach, California, 1933	NVL1	0.41	59
Long Beach, California, 1933	NVL2	0.37	59
San Fernando, California, 1971	NVL3	0.52	38
San Fernando, California, 1971	NVL4	0.61	38
San Fernando, California, 1971	NVL5	0.63	40
Loma Prieta, California, 1989	NVL6	0.53	95
Loma Prieta, California, 1989	NVL7	0.45	97
Loma Prieta, California, 1989	NVL8	0.52	97
Mexico City, 1985	NVL10	0.41	379
Mexico City, 1985	NVL11	0.50	379
Mexico City, 1985	NVL12	0.35	469
Tangshan, China, 1976	NVL13	0.58	373
Imperial Valley, California, 1940	NI1	1.04	8
Kern Country, California, 1940	NI2	1.01	56
Kern Country, California, 1940	NI3	0.99	56
Borrego Mtn., California, 1968	NI4	1.10	122
Borrego Mtn., California, 1968	NI6	1.11	24
San Fernando, California, 1971	NI7	1.01	39
*Coyote Lake, California, 1971	NI8	1.04	5
*Whitier, California, 1987	NI9	0.93	21.5
*Alaskan Subd. Zone, 1983	NI10	0.99	13
Near E. Coast of Honshu, Japan, 1971	NI11	0.97	196
*Near E. Coast of Honshu, Japan, 1971	NI12	1.15	38
Montenegro, Yugoslavia, 1979	NI15	1.19	17
Parkfield, California, 1966	NH1	1.86	7
Parkfield, California, 1966	NH2	1.70	5
San Francisco, California, 1957	NH4	2.28	17
*Helena, Montana, 1935	NH5	2.03	8
*Oroville, California, 1971	NH7	1.91	13
San Fernando, California, 1971	NH8	1.86	34
*Alaskan Subd. Zone, 1986	NH10	1.90	135
*Nahanni N.W.T., Canada, 1985	NH11	2.39	7.5
*Near E. Coast of Honshu, Japan, 1972	NH13	2.43	33
Near E. Coast of Honshu, Japan, 1972	NH14	2.43	116
Friuli, Italy, 1976	NH15	1.79	16

REFERENCES

Aiken, I. D., and Kelly, J. M., 1990. *Earthquake Simulator Testing and Analytical Studies of Two Energy—Absorbing Systems for Multistory Structures, Report No. UCB/EERC-90/03*, University of California, Berkeley, CA.

American Society of Civil Engineers (ASCE), 2000. *Prestandard and Commentary for the Seismic Rehabilitation of Buildings*, prepared for the SAC Joint Venture, published by the Federal Emergency Management Agency, *FEMA-356*, Washington D. C.

Associate Committee on National Building Code, 1995. *National Building Code of Canada 1995*, National Research Council, Ottawa.

Carr, A. J., 2000. *RUAUMOKO—Inelastic Dynamic Analysis* (Users Manual), Department of Civil Engineering, University of Canterbury.

Chopra, A. K., Goel, R. K., and Chintanapakdee, C., 2001. *Statistics of SDF-System Estimate of Roof Displacement for Pushover Analysis of Buildings, PEER Report 2001/16*, Pacific Earthquake Engineering Research Center, University of California, Berkeley.

Constantinou, M. C., Reinhorn, A. M., Mokha, A., and Watson, R., 1991. Displacement control device for base-isolated bridges, *Earthquake Spectra* **7** (2), 179–200.

Constantinou, M. C., Soong, T. T., and Dargush, G. F., 1998, *Passive Energy Dissipating Systems for Structural Design and Retrofit*, MCEER, University of New York at Buffalo, Buffalo, NY.

Filiatrault, A., and Cherry, S., 1987. Comparative performance of friction damped systems and base isolation systems for earthquake retrofit and seismic design, *Earthquake Eng. Struct. Dyn.* **16**, 389–416.

Filiatrault, A., and Cherry, S., 1989. Efficient numerical modelling for the design of friction damped braced steel plane frames, *Can. J. Civ. Eng.* **16**, 211–218.

Filiatrault, A., and Cherry, S., 1990. Seismic design for friction-damped structures, *J. Struct. Eng.* **116** (5), 1334–1355.

FitzGerald, T. F., Anagnos, T., Goodson, M., and Zsutty, T., 1989. Slotted bolted connections in aseismic design for concentrically braced connections, *Earthquake Spectra* **5** (2), 383–391.

Fu, Y., and Cherry, S., 2000. Design of friction damped structures using lateral force procedure, *Earthquake Eng. Struct. Dyn.* **29** (7), 989–1010.

Gluck, N., Reinhorn, A. M., Gluck, J., and Levy, R., 1996. Design of supplemental dampers for control of structures, *J. Struct. Eng.* **122** (12), 1394–1399.

Hanson, R. D., and Soong, T. T., 2001. *Seismic Design with Supplemental Energy Dissipation Devices*, monograph, Earthquake Engineering Research Institute, Oakland, CA.

Heidebrecht, A. C., and Lu, C. Y., 1988. Evaluation of the seismic response factor introduced in the 1985 edition of the National Building Code of Canada, *Can. J. Civ. Eng.* **15**, 382–388.

Kitajima, K., Ageta, N., Nakanishi, M., and Adachi, N., 1997. Pseudo-dynamic test on reinforced concrete frame retrofitted with damper, *Trans. Jpn. Concr. Inst.* **19**, 203–210.

Krawinkler, H., and Seneviratna, G. D. P. K., 1998. Pros and cons of a pushover analysis of seismic performance evaluation, *Eng. Struct.* **20** (4–6), 452–464.

Levy, R., Marianchik, E., Rutenberg, A., and Segal, F., 2001. A simple approach to the seismic design of friction damped medium-rise frames, *Eng. Struct.* **23** (3), 250–259.

Naumoski, N., Heidebrecht, A. C., and Rutenberg, A., 1993. *Representative Ensembles of Strong Motion Earthquake Records, EERG Report 93-1*, Earthquake Engineering Research Group, McMaster University, Hamilton, Ontario.

Nims, D. K., Richter, P. J., and Bachman, R. E., 1993. The use of the energy dissipating restraint for seismic hazard mitigation, *Earthquake Spectra* **3** (9), 467–489.

Ohnishi, H., Kitajima, K., Nakanishi, M., and Adachi, N., 1999. A study on friction dampers for response-control retrofit of existing R/C buildings, *Trans. Jpn. Concr. Inst.* **21**, 439–446.

Pall, A. S., and Marsh, C., 1982. Response of friction damped braced frames, *J. Struct. Div. ASCE* **108**, 1313–1323.

Pall, A. S., and Pall, R., 1996. Friction dampers for seismic control of buildings—A Canadian experience, *Proceedings of 11th World Conference on Earthquake Engineering, Acapulco, Mexico, June 23–28*, Elsevier Science Ltd., Paper No. 497.

Popov, E. P., Yang, T. S., and Grigorian, C. E., 1993. New directions in structural seismic designs, *Earthquake Spectra* **9** (4), 845–875.

Rao, R. S., Gergely, P., and White, R. N., 1996. A simplified design method for retrofit of gravity load design RC frames with friction dampers, *Proceedings of 11th World Conference on Earthquake Engineering, Acapulco, Mexico, June 23–28*, Elsevier Science Ltd., Paper No. 1691.

Singh, M. P., and Moreschi, L. M., 2001. Optimal seismic design of building structures with friction dampers, *Proceedings of Earthquake Engineering Frontiers in the New Millennium: Proceedings of the China-U. S. Millennium Symposium on Earthquake Engineering, Beijing, 8–11 November 2000*, A. A. Balkema, Lisse, The Netherlands, pp. 345–350.

Tremblay, R., and Stiemer, S. F., 1993. *Proceedings of Seminar on Seismic Isolation, Passive Energy Dissipation and Active Control*, Applied Technology Council, *ATC 17-1*, Vol. 2, San Francisco, CA.

Vulcano, A., 1995. Design of damped steel bracing systems for seismic control of framed structures, *Proceedings of 10th European Conference on Earthquake Engineering, Vienna*, Vol. 3, pp. 1567–1572.

Way, D., and Taylor, B., 1996. Seismic retrofit of the TransWorld Bank building using friction dampers for energy dissipation, *Proceedings of Passive Energy Dissipation Systems for New and Existing Buildings Symp., Alhambra, Calif.*

(Received 18 January 2001; accepted 21 October 2004)